Plant Ecology (2005) 179:133–147
DOI 10.1007/s11258-004-4641-6

Spatial associations and patterns of perennial vegetation in a semi-arid steppe: a multivariate geostatistics approach

Fernando T. Maestre[1,2,*], Francisco Rodríguez[3], Susana Bautista[1,4], Jordi Cortina[1] and Juan Bellot[1]

*[1]Departamento de Ecología, Universidad de Alicante, Apartado de Correos 99, 03080 Alicante, Spain; [2]Present address: Department of Biology, Duke University, Phytotron Building, Science Drive, Box 90340, Durham, North Carolina 27708-0340, USA; [3]Departamento de Matemática Aplicada, Universidad de Alicante, Apartado de Correos 99, 03080 Alicante, Spain; [4]Centro de Estudios Ambientales del Mediterráneo (CEAM), C/ Charles Darwin, 14, 46980 Paterna, Spain; *Author for correspondence (e-mail: maestre@duke.edu; phone: +1-9196607406; fax: +1-9196607425)*

Received 04 December 2003; acccepted in revised form 29 September 2004

Key words: Linear model of coregionalization, Mediterranean, Scale, Size of sampling units, Spatial pattern, *Stipa tenacissima*

Abstract

We investigated the spatial patterns of perennial species (*Stipa tenacissima*, *Anthyllis cytisoides*, *Globularia alypum*, *Brachypodium retusum* and chamaephytes) in a 50 m × 50 m semi-arid steppe by using the combination of a linear model of coregionalization (LMC) and sampling units of varying size (1.25 m × 1.25 m, 2.5 m × 2.5 m, and 5 m × 5 m). The data-adjusted LMC showed the patchy structure of the vegetation, which was especially evident with the highest resolution grid. It also detected a periodic pattern in the distribution of *S. tenacissima*, as well as autocorrelation at two spatial scales for *A. cytisoides* and *G. alypum*. The latter species was negatively associated with the other species at both short and long distances. These negative associations were consistent for all sampling grids and suggest the presence of interference between *G. alypum* and the rest of the evaluated species. Despite species-specific differences, the LMC was fitted satisfactorily to all of them. This suggests a common variation pattern for all the species, which may be caused by an underlying environmental property driving the patterns of all the species or, alternatively, by the dominance of some species' spatial pattern, or another kind of species association, over the rest. The spatial patterns found were profoundly affected by the observational scale. Our results reveal that the multivariate geostatistical approach introduced in this paper is a suitable technique for the spatial analysis of semi-arid plant communities. It allows plant ecologists to evaluate if the species forming the plant community of interest share a common spatial pattern, and to assess the spatial covariation between the species forming a plant community at different spatial scales independently.

Introduction

The spatial pattern of a plant community is determined by a combination of processes that include soil heterogeneity (Ehrenfeld et al. 1997), biotic interactions (Callaway 1995), patterns of growth and seed dispersal (Lechowicz and Bell 1991), microsite availability for seeds (Harper et al. 1965), and random factors (Halpern 1988). Despite it is not possible to determine the specific

processes involved in the creation of a given plant pattern by looking at its spatial distribution alone (Shipley and Keddy 1987), spatial pattern analysis can provide useful information to infer the underlying formative processes. Thus, it is not surprising that spatial pattern analysis has received substantial attention by plant ecologists in the last decades (Dale 1999), and that numerous methods for quantifying spatial patterns have been developed (Perry et al. 2002).

For data collected by means of transects or contiguous quadrats, the so-called block-variance methods, in which a measure of variance is plotted against the block size or the distance between samples – with the peaks indicating the scale of the pattern, – have been widely used during decades (Greig-Smith 1983). When the data are in the form of spatially referenced individuals, methods such as Ripley's *K*-analysis have often been preferred (Haase 1995). Although not as popular as those mentioned above, other methods based on data autocorrelation have been used to describe the spatial structure of individual plant species (Verdú and García-Fayos 1998) and communities (Anand and Kadmon 2000). In the latter case, the most common approach is to summarize the whole plant community using ordination techniques, and then to apply autocorrelation analyses to the ordination scores. Autocorrelation methods have rarely been used for direct comparisons of the joint spatial variation of species within a community. These analyses can be done with a linear model of coregionalization (LMC), a multivariate geostatistical technique based on modeling individual and joint patterns by using a linear combination of single spatial structures (Goovaerts 1992, 1997; Webster et al. 1994).

A crucial issue when studying the spatial patterns of ecological phenomena is scale, which refers primarily to 'grain' – the size or spatial resolution of the sampling unit- and 'extent' – the size of the study area – (Qi and Wu 1996). The importance of scale in ecological research has been increasingly emphasized in light of hierarchy theory, which establishes that ecological systems are complex units consisting of subsystems that are in turn composed of their own subsystems (Allen and Star 1982; Levin 1992; Wu and Loucks 1995). Because loose vertical and horizontal coupling in structure and function among subsystems, these can be separated and studied according to their temporal or spatial scales (or both; Wu 1999). Another important property of spatial heterogeneity, its scale multiplicity in space (e.g., Wu and Loucks 1995; Werner 1999), implies that the spatial patterns observed in the field and the processes that promote them are dependent on the scale of observation (Wu et al. 2000). Studies devoted to analyze plant spatial patterns typically use an *a priori* scale of observation, i.e. a single grain and extent, which is often pre-set by researchers based on previous knowledge (Greig-Smith 1983). Such approach may lead to inappropriate interpretations when the scale of observation does not match the relevant scale at which the processes under study are acting (Wu et al. 2000). The identification and characterization of spatial patterns across a range of scales is an approach commonly employed in disciplines like landscape ecology, geography and remote sensing (Turner et al. 1989; Qi and Wu 1996; Wu 1999; Wu et al. 2000). However, it has barely been used when studying plant spatial patterns (but see He et al. 1994 and Bellehumeur et al. 1997), despite it has often been recommended (Levin 1992) and is critical to accurately interpret the spatial patterns observed in the field (Wu et al. 2000; Wu 2004).

In this study we evaluate the spatial pattern of perennial vegetation in a *Stipa tenacissima* steppe at different spatial scales. These steppes constitute one of the most important vegetation types in the semi-arid areas of the Mediterranean Basin (Le Houérou 2001). Vegetation in *S. tenacissima* steppes is often structured in a spotted or banded spatial configuration, and their spatial patterns resemble those found in semi-arid regions throughout the globe (Valentin et al. 1999). In these steppes, plant spatial patterns have a crucial role in runoff generation and infiltration, soil stability and nutrient cycling, and thus greatly affect their composition, function and dynamics (Puigdefábregas et al. 1999; Maestre and Cortina 2004). Despite its importance, few studies have explored the spatial pattern of perennial vegetation in these steppes, especially at the plant community level (Puigdefábregas and Sánchez 1996; Maestre and Cortina 2002; Webster and Maestre 2004). The main objectives of this paper were to: (i) explore the spatial patterns of the dominant species in a semi-arid *S. tenacissima* steppe, (ii) evaluate their joint spatial variation, and (iii) assess how these patterns are affected by

changing the scale of observation, i.e. by changing grain size. To achieve these objectives, we used the combination of a multivariate geostatistical approach (LMC) and sampling units of varying size.

Methods

Study area

The study site is a *S. tenacissima* steppe located near Aigües de Busot (38°31′ N, 0°21′ W, 460 m above sea level, 12° slope, 160° SE aspect), 35 km NE of Alicante (SE Spain). The site is representative of this type of steppes in the western Mediterranean, and has been the subject of several previous studies (e.g., Maestre and Cortina 2002; Maestre et al. 2002, 2003; Webster and Maestre 2004). The climate is semi-arid, with a mean annual rainfall of 388 mm and a mean annual temperature of 15.8 °C (closest meteorological station: Relleu, 10 km N). The dry season lasts from May to September, and there is a large interannual variation in rainfall amount and concentration. Soils are loamy-silty loam, *Lithic Calciorthid* (Soil Survey Staff 1990). Vegetation is dominated by the perennial grasses *S. tenacissima* and *Brachypodium retusum*; shrubs like *Globularia alypum*, *Anthyllis cytisoides* and *Ephedra fragilis* (nomenclature following Mateo and Crespo 1998) are also present.

Field sampling

During spring 1999, one 50 m × 50 m plot was established in the center of the study area. The outlines of the canopies of the perennial vegetation within this plot were established visually and fully mapped in the field. To reduce errors during mapping we marked with 1 m-height sticks the corners of nested subplots of 5 m × 5 m and 1 m × 1 m; the latter were used as reference units for mapping. To avoid an excessive number of classes, the chamaephytes (*Fumana ericoides*, *Fumana thymifolia*, *Thymus vulgaris*, *Thymus moroderi*, *Teucrium carolipaui* and *Teucrium capitatum* subsp. *gracillinum*) were grouped into one class (thereafter chamaephytes). Field maps of all the subplots were scanned, assembled into a continuous map, digitized using Adobe Photoshop 5.0 (Adobe Systems Inc., San José, CA, USA) and translated into a GIS, the Idrisi system (Clark University, Worcester, MA, USA). The resulting map is shown in the Appendix 1.

With the aim of exploring the effect of the scale of observation on the spatial patterns observed, we divided the map in quadrats of 1.25 m × 1.25 m, 2.5 m × 2.5 m, and 5 m × 5 m, resulting in sampling square grids of 1600, 400 and 100 quadrats respectively. Using the GIS we calculated the cover of each species for each quadrat, and we obtained the percent cover by dividing the cover area of each species by the total area of the quadrat. This was taken as our raw data. In this paper we present data for *S. tenacissima*, *G. alypum*, *B. retusum*, *A. cytisoides* and the chamaephytes, which represent more than 90% of the total plant cover.

Spatial analysis of individual species

To characterize the spatial pattern of each species we used the semivariogram. We computed experimental semivariograms according to the usual estimator (Webster and Oliver 1990):

$$\hat{\gamma}(\mathbf{h}) = \frac{1}{2N(\mathbf{h})} \sum_{i=1}^{N(\mathbf{h})} \{z(\mathbf{x}_i) - z(\mathbf{x}_i + \mathbf{h})\}^2$$

where $z(\mathbf{x}_i)$ and $z(\mathbf{x}_i + \mathbf{h})$ are the observed cover values of a given species at locations $\mathbf{x}_i$ and $\mathbf{x}_i + \mathbf{h}$, respectively, $\mathbf{h}$ is the lag between samples and $N(\mathbf{h})$ is the number of paired comparisons at lag $\mathbf{h}$. We used omnidirectional semivariograms $\hat{\gamma}(h)$, functions of the lag distance $h = |\mathbf{h}|$. To allow for better comparisons of the different species, all the semivariograms were standardized (Rossi et al. 1992) by dividing each semivariogram value by the variance at that lag (Pannatier 1997). Although cover data were positively skewed, exploratory analysis confirmed that the spatial structure revealed by the standardized semivariograms did not show differences from that revealed by more robust measures of autocorrelation, such as the madogram (Pannatier 1997) and relative semivariograms (Isaaks and Srivatsava 1989).

We fitted two different isotropic models to the experimental semivariograms according to the major spatial patterns observed in the data: short-range autocorrelation or short- and long-range autocorrelation. To describe the first case we used a spherical model with a nugget effect (Webster and Oliver 1990):

$$\gamma(0) = 0$$

$$\gamma(h) = C_0 + C\left\{\frac{3h}{2a} - \frac{1}{2}\left(\frac{h}{a}\right)^3\right\} \quad \text{for } 0 < h \leq a$$

$$\gamma(h) = C_0 + C \quad \text{for } h > a$$

where C_0 is the nugget – the amount of variance not accounted for the model due to measurement error plus residual variation at distances less than the shortest sampling interval, C is the structural variance – part of the total variance that can be attributed to the spatial autocorrelation, and a is the range, which represents the distance beyond which samples are spatially independent (Webster and Oliver 1990). In this model, the sill (the plateau that the variogram reaches at the range) is $C_0 + C$. When both short and long ranges were detected in the semivariogram, we fitted a nested spherical model with a nugget effect (Webster and Oliver 1990):

$$\gamma(0) = 0$$

$$\gamma(h) = C_0 + C_1\left\{\frac{3h}{2a_1} - \frac{1}{2}\left(\frac{h}{a_1}\right)^3\right\} + C_2\left\{\frac{3h}{2a_2} - \frac{1}{2}\left(\frac{h}{a_2}\right)^3\right\} \quad \text{for } 0 < h \leq a_1$$

$$\gamma(h) = C_0 + C_1 + C_2\left\{\frac{3h}{2a_2} - \frac{1}{2}\left(\frac{h}{a_2}\right)^3\right\} \quad \text{for } a_1 < h \leq a_2$$

$$\gamma(h) = C_0 + C_1 + C_2 \quad \text{for } h > a_2$$

where C_0 is the nugget, and C_1 and C_2 indicate the value of structural variance for the first (a_1) and second (a_2) range structures respectively. In this model the sill is $C_0 + C_1 + C_2$.

For all the fitted models, we used the proportion of the model sample variance explained by structural variance, $(C_1 + C_2)/(C_0 + C_1 + C_2)$, as a normalized measure of spatial dependence (Robertson and Freckman 1995). We computed experimental semivariograms with Variowin 2.2 (Pannatier 1997). Each semivariogram lag class had at least 684, 2964 and 9948 pairs of points for the 5 m × 5 m, 2.5 m × 2.5 m, and 1.25 m × 1.25 m grids, respectively. We fitted all the experimental semivariograms to spherical and nested-spherical modes following a weighted least-squares approximation (Cressie 1985). We assigned weights according to the number of paired comparisons in the estimates, and selected for each species and grain size the model with the smallest residual mean square (Webster and Oliver 1990).

Joint spatial analysis by coregionalization

To explore the spatial covariation between the species studied we used a LMC, following the theory presented in Goovaerts (1992) and Webster et al. (1994). The idea underlying this analysis is that processes with various spatial structures that act additively generate the spatial pattern of a species. It implies that the form of all individual and cross-semivariograms (see below) is that of a nested model composed of the same elementary semivariogram functions, but weighted by specific components (Goulard and Volz 1992). The LMC was performed in three steps:

(i) Estimation of the $p(p + 1)/2$ experimental individual and cross-semivariograms, where p is the number of species present in the data. If the cover of the two species to be compared, u and v, are denoted as $z_u(\mathbf{x})$ and z_v $(\mathbf{x})$, the cross-semivariogram, $\gamma_{uv}(\mathbf{h})$, can be estimated by the following equation (Webster et al. 1994):

$$\hat{\gamma}_{uv}(\mathbf{h}) = \frac{1}{2N(\mathbf{h})}\sum_{i=1}^{N(\mathbf{h})}\{z_u(\mathbf{x}_i) - z_u(\mathbf{x}_i + \mathbf{h})\} \times \{z_v(\mathbf{x}_i) - z_v(\mathbf{x}_i + \mathbf{h})\}$$

(ii) Selection of the number and characteristics (type of function and range) of the basic semivariogram functions to be fitted to all individual and cross-semivariograms. To perform this selection, we computed semivariograms of the scores of the leading components of a Principal Components Analysis (PCA) applied to the cover values from all species for each of the three grids under study. The first two axes of this PCA accounted for 58%, 53% and 50% of the variation in the data for the 5 m × 5 m, 2.5 m × 2.5 m, and 1.25 m × 1.25 m grids, respectively. Using these semivariograms, we modeled the whole set of individual and cross-semivariograms by using the following nested spherical model with nugget:

$$\gamma_{uv}(0) = 0$$

$$\gamma_{uv}(h) = b^1_{uv} + b^2_{uv}\left\{\frac{3h}{2a_1} - \frac{1}{2}\left(\frac{h}{a_1}\right)^3\right\} + b^3_{uv}\left\{\frac{3h}{2a_2} - \frac{1}{2}\left(\frac{h}{a_2}\right)^3\right\} \quad \text{for } 0 < h \leq a_1$$

$$\gamma_{uv}(h) = b^1_{uv} + b^2_{uv} + b^3_{uv}\left\{\frac{3h}{2a_2} - \frac{1}{2}\left(\frac{h}{a_2}\right)^3\right\} \quad \text{for } a_1 < h \leq a_2$$

$$\gamma_{uv}(h) = b^1_{uv} + b^2_{uv} + b^3_{uv} \quad \text{for } h > a_2$$

where a_1 and a_2 are the first and second ranges respectively. Using the models fitted to the scores of the first two components of the PCA (Table 1), we selected the values of a_1 and a_2 for each sampling grid. In these equations, b^k_{uv}, where $k = 1$, 2 and 3, are coefficients to be obtained from the data. For each k, the matrix of the coefficients b^k_{uv} is called the coregionalization matrix, $\mathbf{B}^k$. The LMC requires these matrices to be positive semidefinite, i.e. that its determinant and all its principal minor determinants are non-negative (Goovaerts 1992).

(iii) Fitting the selected model to the experimental individual and cross-semivariogram values under the constraint of positive semi-definiteness of the matrix of coefficients, $\mathbf{B}^k$. We did it by using the iterative algorithm described in Goulard and Volz (1992). This algorithm starts with a set of initial matrices $\mathbf{B}^k$, and modify one matrix at a time iteratively so as to minimize the weighted sum of squares of the differences between the experimental and model cross-semivariogram values, under the constraint that the matrix of the coefficients is positive semidefinite. Further details on the procedure, and the complete set of equations of the algorithm used, can be found in Goovaerts (1997).

Principal component analyses were performed with SPSS for Windows 9.0 (SPSS Inc., Chicago, USA). Cross-semivariograms were computed with Variowin 2.2 (Pannatier 1997). The selected model was fitted to cross-semivariograms with a Maple (Waterloo Maple Inc., Waterloo, Canada) procedure implementing the algorithm of Goulard and Volz (1992).

Comparison of the spatial patterns between pairs of species

As a first approach to evaluate the main differences in pattern relationships between pairs of species and sampling grids, we computed Pearson correlation coefficients with cover values. For a given sampling unit, the sum of specific cover frequencies cannot exceed the value of 1. Thus, negative correlations between pairs of species can be expected, and correlation coefficients must be interpreted in relative terms by comparing them with the expected coefficients calculated as a function of the species cover values. We computed the expected correlations assuming a Dirichlet (multivariate Beta) distribution (Kotz et al. 2000), and we used them as indicator values for comparison purposes. The expected correlations were calculated with the equation:

$$-\sqrt{\frac{p_i p_j}{(1-p_i)(1-p_j)}}$$

where p_i and p_j are cover values for the i and j species respectively.

Table 1. Parameters of the models fitted to the standardized semivariograms of the scores of the first two components of a principal components analysis (PCA) performed with raw cover values.

Grid	PCA Axis	Model	C_0	C_1	C_2	a_1	a_2
5 m × 5 m	1	Nested spherical	0.17	0.38	0.57	16.5	30
	2	–[a]	–	–	–	–	–
2.5 m × 2.5 m	1	Spherical	0.45	0.55	–	6.5	–
	2	Spherical	0.49	0.60	–	25	–
1.25 m × 1.25 m	1	Spherical	0.30	0.69	–	4	–
	2	Nested spherical	0.36	0.49	0.21	4	29

[a]There is no apparent spatial structure at this scale. We could not fit any model. C_0 = nugget variance, a_1 = first range, a_2 = second range, C_1 = structural variance for the first range, C_2 = structural variance for the second range.

A more powerful approach to compare the spatial patterns of the different species within a plant community can be obtained with the coregionalization matrix, $\mathbf{B}^k$. This matrix gives useful information about the spatial relationships between the species under study, since it describes these relationships at the spatial scale defined by the corresponding basic semivariogram function: nugget ($k = 0$), spherical with range a_1 ($k = 1$) and spherical with range a_2 ($k = 2$). From this matrix, the structural correlation coefficient (r^k_{uv}) is defined as:

$$r^k_{uv} = \frac{b^k_{uv}}{\sqrt{b^k_{uu} b^k_{vv}}}$$

With r^k_{uv} we can distinguish between the correlation structures encountered at each of the different spatial scales of the fitted nested model (nugget, first and second range) separately, filtering out the structures belonging to other scales of variation. This facilitates the comparison of the spatial patterns of the different species. With the aim of summarizing the relationships between species, we applied a PCA to the coregionalization matrices obtained for the three grids under study, and projected the variables into correlation circles as explained in Webster et al. (1994). To perform this, the eigenvectors from the two leading principal components were converted to the correlations between the original variables and the principal components with the equation:

$$c^k_{ij} = a_{ij}\sqrt{\frac{\lambda_j}{b^k_{ii}}}$$

where c^k_{ij} is the value of the correlation, k refers to each of the matrices defined in the LMC (nugget, first and second range), a_{ij} is the i th element of the jth eigenvector, λ_j is the j th eigenvalue, and b^k_{ii} is the k element corresponding to the ith species. These correlations were plotted in the unit circle in the plane of the principal components. We applied the same analysis to the variance–covariance matrix of the original variables. PCA analyses were performed with SPSS for Windows 9.0 (SPSS Inc., Chicago, USA).

Results

The total plant cover of the plot studied was 46%; it contained 1720 plant patches – spatially discrete units of the different species – (Appendix 1). *Brachypodium retusum* and *S. tenacissima* were the dominant species in the community, with cover values of 17.4% (393 patches) and 16.6% (383 patches), respectively. *Globularia alypum* had a low cover value (5.1%), despite it had the highest number of patches (405). *Anthyllis cytisoides* had 1.7% of cover and 229 patches. The chamaephytes were the least represented group on the study site, with a cover of 0.8% and 141 patches.

The experimental semivariograms revealed a clear spatial structure for most species and grain sizes, with *G. alypum* and the chamaephytes having the most and the least structured semivariograms, respectively (Figure 1). The spatial structures of *B. retusum* and *S. tenacissima* were best captured by the semivariograms as we moved from the 1.25 m × 1.25 m to the 5 m × 5 m grids. This was not the case for *G. alypum*. For this species, reducing grain size allowed us to detect the presence of a short range of 3–4 m in the 2.5 m × 2.5 m and 1.25 m × 1.25 m grids, which was not detected in the 5 m × 5 m grid. The semivariograms for *S. tenacissima* showed a clear dip at about 16 m, especially evident with the 2.5 m × 2.5 m grid. The models fitted independently to the semivariograms estimated moderate to high spatial dependence for *S. tenacissima*, *B. retusum* and *G. alypum*, regardless of grain size (Table 2). The values of spatial dependence for the chamaephytes and *A. cytisoides* were moderate for the smallest grain size, but they became substantially reduced or even disappeared in the largest grain size. For *S. tenacissima* and *B. retusum*, the semivariograms detected similar patterns, sharing an increase in semivariance with lag distance up to a range of 4–10 m, depending on grain size. *Globularia alypum* showed a strong spatial structure regardless of grain size, with a range up to 25 m. As with *G. alypum*, the semivariograms revealed the presence of a short range in *A. cytisoides* at the 2.5 m × 2.5 m and 1.25 m × 1.25 m grids, which was not evident at the 5 m × 5 m one. This species showed autocorrelation up to 17 m. The chamaephytes showed a random pattern at the largest grain size. At higher resolutions, they presented ranges varying from 5 m to 1 m.

The LMC chosen was well fitted to all the experimental semivariograms (Figure 1) and cross-semivariograms (Figures 2, 3 and 4). The negative relationship between the patterns of *S. tenacissima* and *B. retusum* showed a 'pure nugget' effect when

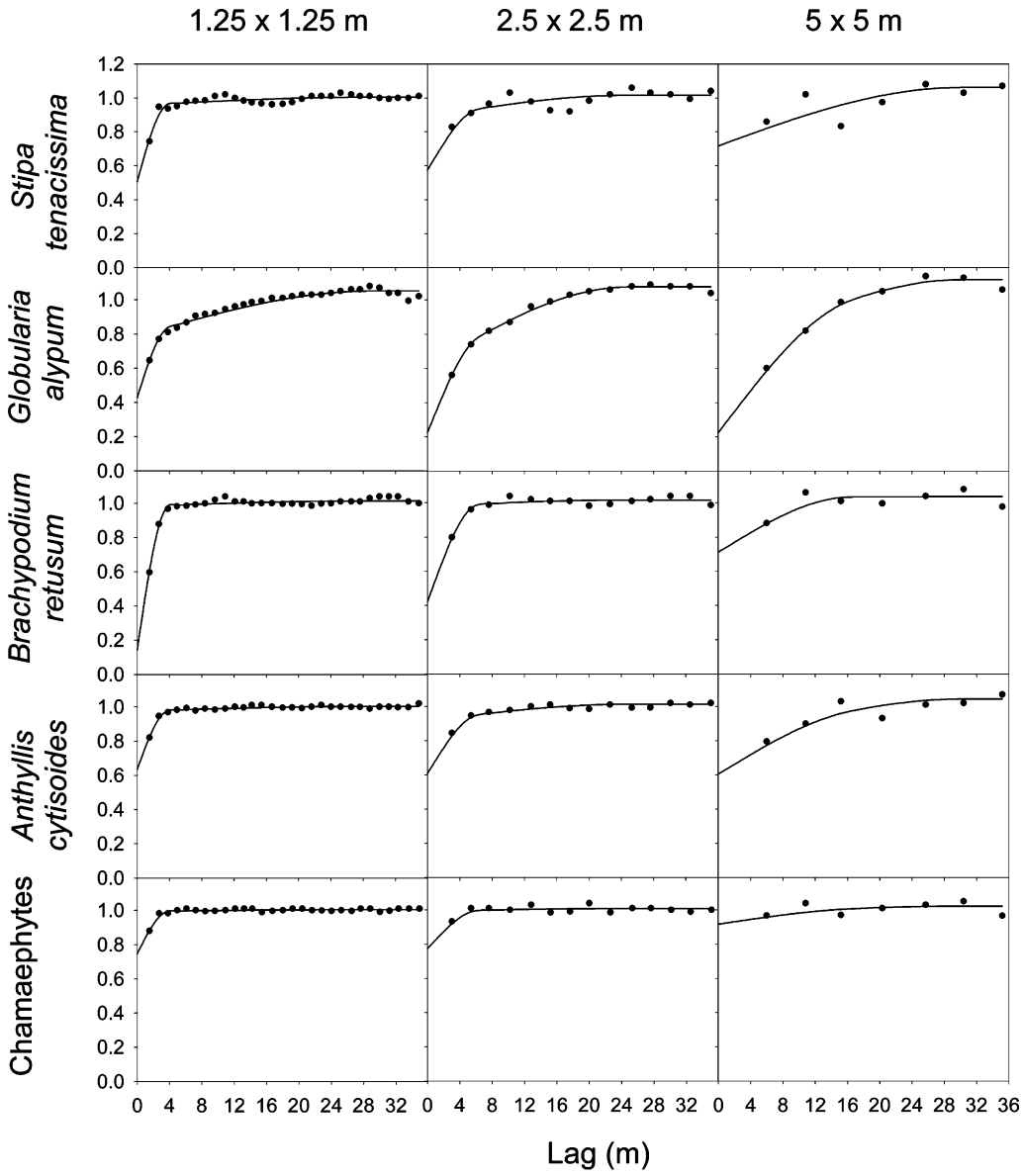

Figure 1. Experimental semivariograms (dots) and coregionalization model fitted (solid line) for the three sampling grids. Note that the models fitted are not those fitted individually to each semivariogram, which are described in Table 2.

using the 5 m × 5 m grid (Figure 2); the nugget component disappeared to zero when using the 1.25 m × 1.25 m grid (Figure 4). This suggests that the negative correlation structure of these species was mainly associated to short distances. The cross-semivariograms between *G. alypum* and the remaining species consistently showed strong negative relationships that increased with distance up to 16–28 m. On the contrary, the cross-semivariograms between *A. cytisoides* and the remaining species – except *G. alypum* – revealed some positive relationships, mainly with *B. retusum* at the 5 m × 5 m grid. With this grain size, the sign of the correlation between the spatial increments in *S. tenacissima* and *A. cytisoides* shifted from the shortest to the largest distances (Figure 2).

The observed correlations between *G. alypum* and the remaining species were more negative than expected in all the sampling grids (Table 3). Contrarily, the observed correlations between

Table 2. Parameters of the models fitted to the standardized semivariograms of evaluated species.

Species	Size of sampling units	Model	C_0	C_1	C_2	a_1	a_2	SPD
S. t.	5 m × 5 m	Spherical	0.33	0.66	–	9.96	–	66.73
	2.5 m × 2.5 m	Spherical	0.59	0.41	–	8.28	–	41.00
	1.25 m × 1.25 m	Spherical	0.57	0.41	–	4.29	–	41.84
G. a.	5 m × 5 m	Spherical	0.28	0.87	–	25.20	–	75.65
	2.5 m × 2.5 m	Nested spherical	0.03	0.53	0.52	4.68	23.40	77.78
	1.25 m × 1.25 m	Nested spherical	0.33	0.51	0.18	3.30	19.14	67.58
B. r.	5 m × 5 m	Spherical	0.06	0.97	–	9.01	–	94.15
	2.5 m × 2.5 m	Spherical	0.45	0.56	–	7.28	–	54.95
	1.25 m × 1.25 m	Spherical	0.10	0.90	–	3.96	–	89.88
A. c.	5 m × 5 m	Spherical	0.56	0.42	–	17.07	–	42.86
	2.5 m × 2.5 m	Nested spherical	0.59	0.30	0.11	5.40	15.48	41.04
	1.25 m × 1.25 m	Nested spherical	0.23	0.73	0.05	2.58	18.48	76.92
C. s.	5 m × 5 m	– [a]	–	–	–	–	–	–
	2.5 m × 2.5 m	Spherical	0.66	0.35	–	5.35	–	34.43
	1.25 m × 1.25 m	Spherical	0.31	0.69	–	2.33	–	68.89

[a]There is no apparent spatial structure at this scale. We could not fit any model. C_0 = nugget variance, a_1 = first range, a_2 = second range, C_1 = structural variance for the first range, C_2 = structural variance for the second range, SPD = spatial dependence (%). S. t. = *Stipa tenacissima*, G. a. = *Globularia alypum*, B. r. = *Brachypodium retusum*, A. c. = *Anthyllis cytisoides*, and C. s. = chamaephytes.

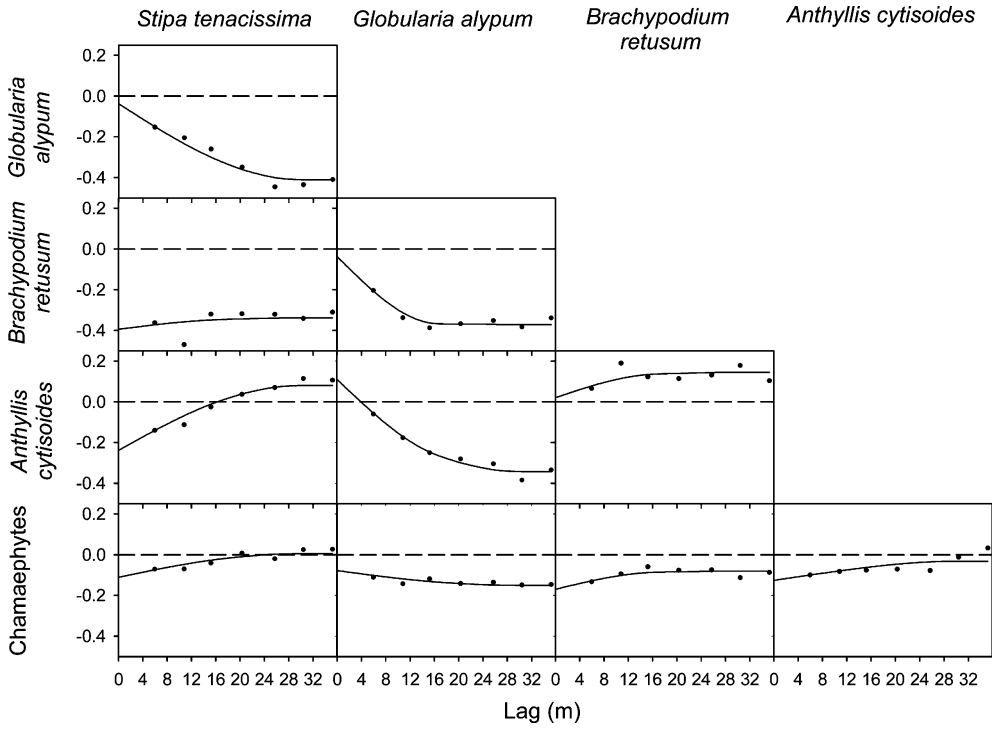

Figure 2. Cross-semivariograms (dots) and model fitted (solid line) for the 5 m × 5 m grid.

A. cytisoides and *B. retusum* were less negative than expected. The structural correlation coefficients from the coregionalization analysis allowed us to analyze separately the correlation structure at each spatial scale, eliminating structures belonging to other scales of variation (Table 4). At the large scale (second range), except for the pairs that included *G. alypum*, the spatial relationships between species were very positively correlated. Thus, correlation circles for the second range, and

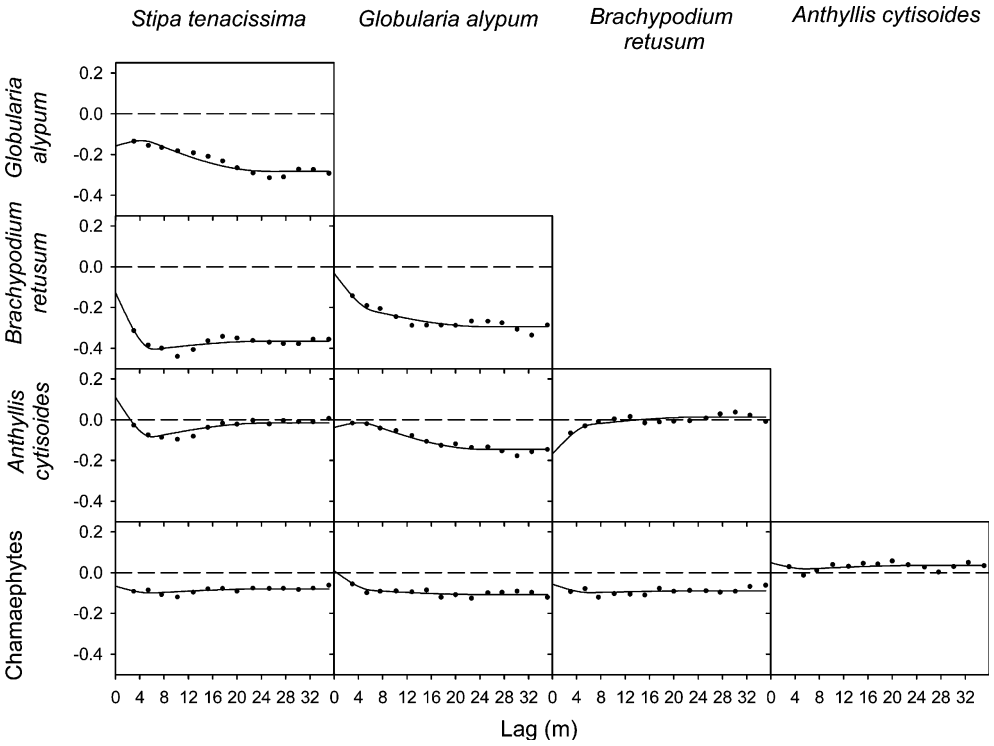

Figure 3. Cross-semivariograms (dots) and model fitted (solid line) for the 2.5 m × 2.5 m grid.

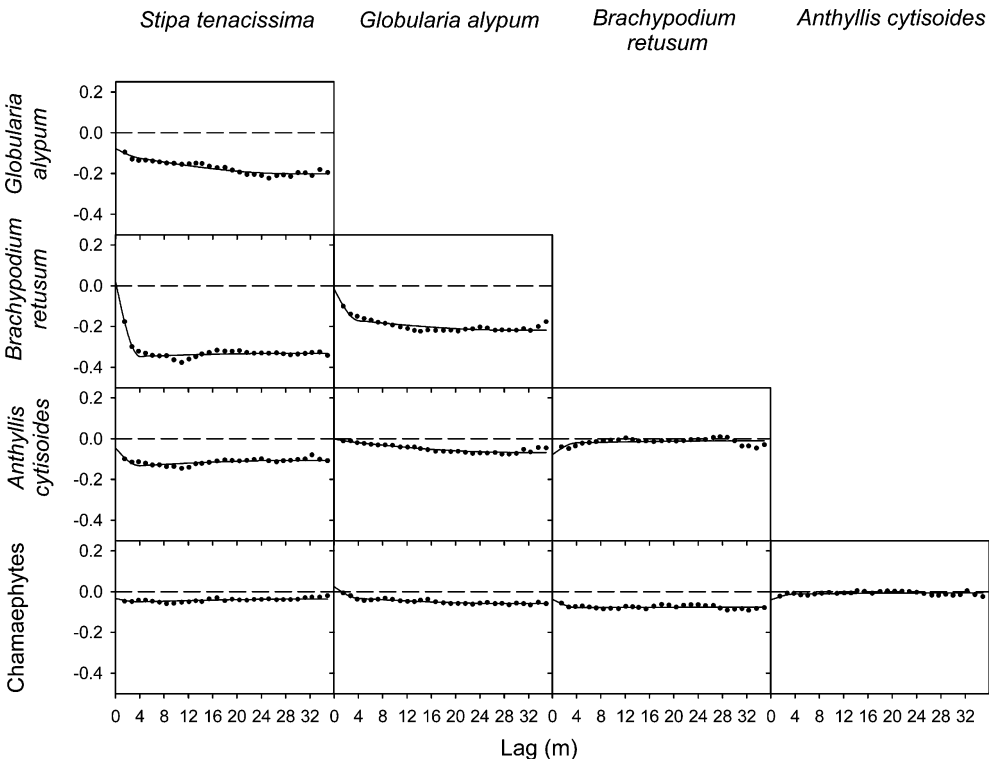

Figure 4. Cross-semivariograms (dots) and model fitted (solid line) for the 1.25 m × 1.25 m grid.

Table 3. Matrix of observed and expected correlations.

	Globularia alypum	*Brachypodium retusum*	*Anthyllis cytisoides*	Chamaephytes
5 m × 5 m grid				
Stipa tenacissima	−0.375	−0.337	0.064	0.022
Globularia alypum		−0.331	−0.295	−0.159
Brachypodium retusum			0.120	−0.091
Anthyllis cytisoides				−0.023
2.5 m × 2.5 m grid				
Stipa tenacissima	−0.270	−0.367	−0.012	−0.073
Globularia alypum		−0.267	−0.137	−0.109
Brachypodium retusum			0.005	−0.086
Anthyllis cytisoides				0.033
1.25 m × 1.25 m grid				
Stipa tenacissima	−0.198	−0.322	−0.096	−0.044
Globularia alypum		−0.210	−0.074	−0.053
Brachypodium retusum			−0.011	−0.073
Anthyllis cytisoides				−0.006
Expected				
Stipa tenacissima	−0.104	−0.205	−0.059	−0.040
Globularia alypum		−0.107	−0.031	−0.021
Brachypodium retusum			−0.061	−0.041
Anthyllis cytisoides				−0.012

Table 4. Matrix of structural correlation coefficients for the three sampling grids.

	1.25 m × 1.25 m grid				2.5 m × 2.5 m grid				5 m × 5 m grid			
	G. a.	B. r.	A. c.	C. s.	G. a.	B. r.	A. c.	C. s.	G. a.	B. r.	A. c.	C. s.
Nugget												
Stipa tenacissima	−0.167	0.083	−0.081	−0.055	−0.438	−0.256	0.186	−0.100	−0.095	−0.552	−0.362	−0.137
Globularia alypum		−0.064	−0.004	0.043		−0.103	−0.103	0.019		−0.096	0.296	−0.172
Brachypodium retusum			−0.263	−0.114			−0.332	−0.099			0.031	−0.210
Anthyllis cytisoides				−0.060				0.070				−0.169
First range												
Stipa tenacissima	−0.069	−0.607	−0.240	−0.059	0.276	−0.727	−0.755	−0.172	−0.234	0.588	0.567	0.760
Globularia alypum		−0.262	−0.016	−0.172		−0.300	0.243	−0.288		−0.858	−0.527	−0.070
Brachypodium retusum			0.105	−0.091			0.297	−0.135			0.401	0.573
Anthyllis cytisoides				0.097				−0.155				−0.074
Second range												
Stipa tenacissima	−0.846	0.483	0.898	0.724	−0.913	0.992	0.999	0.724	−0.911	0.643	0.997	0.722
Globularia alypum		−0.643	−0.695	−0.619		−0.957	−0.920	−0.381		−0.270	−0.874	− 0.373
Brachypodium retusum			0.414	0.124			0.994	0.633			0.704	0.994
Anthyllis cytisoides				0.374				0.712				0.777

G. a. = *Globularia alypum*, B. r. = *Brachypodium retusum*, A. c. = *Anthyllis cytisoides*, and C. s. = chamaephytes.

also for the total coregionalization matrix clearly distinguished between *G. alypum* and the remaining species (Figure 5). At the short scale (first range), the positive relationships between the spatial patterns of *B. retusum* and *A. cytisoides* were highlighted, as were the negative relationships between *S. tenacissima* and *B. retusum* at the smallest grain size. The differences between *G. alypum* and the remaining species were also evident at the spatial scale defined by the first range.

Discussion

Despite the apparent regularity that reportedly characterizes plant spatial patterns in semi-arid

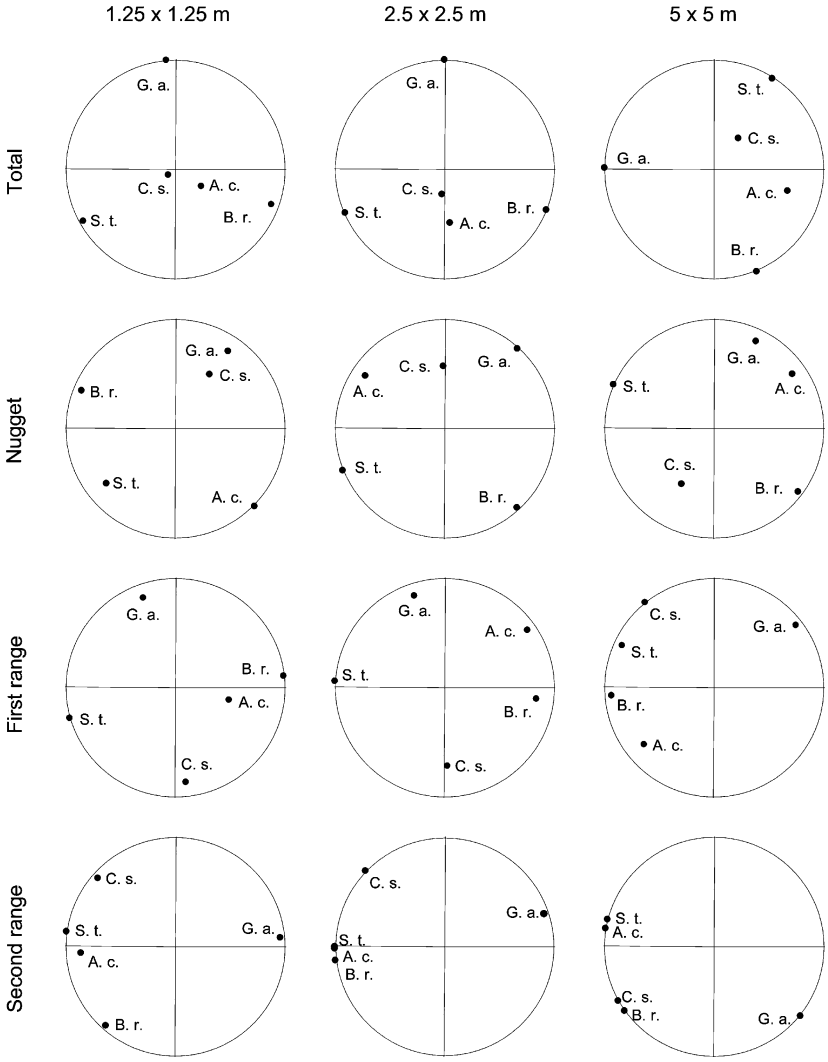

Figure 5. Correlation circles for the three sampling grids employed. S. t. = *Stipa tenacissima*, G. a. = *Globularia alypum*, B. r. = *Brachypodium retusum*, A. c. = *Anthyllis cytisoides*, and C. s. = chamaephytes.

steppes (Valentin et al. 1999), we found that the spatial patterns of perennial vegetation in our study site were quite complex. The semivariograms detected notable differences in the spatial patterns of the different species studied. The most noticeable differences were found between *S. tenacissima* and the rest of species. The dip or 'hole effect' found in the semivariograms of *S. tenacissima* suggests the presence of a regular pattern in the distribution of this species (Webster and Oliver 1990). Puigdefábregas and Sánchez (1996), working in a 4.37 ha study area in Almería (SE Spain), found the same effect in their semivariograms of *S. tenacissima* cover, but in their case the dip occurred at shorter ranges (between 2 and 4 m) than those observed in our study.

The linear model of corregionalization (LMC) allows plant ecologists to evaluate if the species forming the community of interest share a common spatial pattern, and to assess the spatial covariation between the different species at different spatial scales independently by using the structural correlation coefficient. In our study area, the LMC fitted satisfactorily to all species. This suggests a common variation pattern for all the species, which may be caused by an underlying environmental property

driving the patterns of all the species (e.g., large-scale variation in soil properties) or, alternatively, by the dominance of some species' spatial pattern, or another kind of species association, over the rest. However, it also revealed substantial differences in the spatial relationships between the different species studied. The clearest results were found for *G. alypum*; despite being the species with most patches in the steppe studied, it was negatively related to the rest of the species. The LMC showed clearly that these negative associations were consistent for all the sampling grids. However, the mechanisms underlying these patterns can not be elucidated with our study; they may result from seed dispersal, allelophatic interactions – leaves of *G. alypum* are rich in compounds such as flavonoids, glucosids and phenolic acids (Rivera and Obón 1991) – or belowground competition, among other factors. Our results agree with those of Webster and Maestre (2004), who found a negative association between *G. alypum* and the rest of perennial species in two *S. tenacissima* steppes close to our study site. However, they contrast with those of García-Fayos and Gasque (2002), who found a positive association between *G. alypum* and *S. tenacissima* in other steppe. These contrasting results suggest that the relative importance of the mechanisms underlying the interactions between *G. alypum* and other species may differ among sites. Further studies are needed to know these mechanisms, and to test the validity of this affirmation. It is also interesting to note the lack of positive relationships between the chamaephytes and the remaining species; it may be due to the sampling procedure used (grouping of several species in a single category), which may mask existing species-specific patterns.

The spatial patterns of the different species forming the steppe studied were profoundly affected by grain size. The 5 m × 5 m grid did not allow us to detect small-scale aggregations between individuals of *A. cytisoides* and *G. alypum*, and did not reveal any spatial pattern in the distribution of the chamaephytes. The increase in the resolution allowed us to detect small-scale conspecific associations between individuals of *G. alypum* and *A. cytisoides*, suggested by the short-range visible in the semivariograms, and to detect the spatial pattern of the chamaephytes clearly. Such an increase also reduced the ranges in the semivariograms of *S. tenacissima* and *B. retusum*. Grain size also modified the magnitude, and even the sign, of the structural correlation coefficients among pairs of species. We found a positive association between the spatial patterns of *S. tenacissima* and the remaining species when using the 5 m × 5 m grid. However, increasing the resolution allowed us to detect a positive association only between *S. tenacissima* and *A. cytisoides*, but at the distances defined by the second range of the LMC. Thus, this association could reflect the distribution of edaphic or topographic characteristics in the study area, rather than biotic interactions mediated by environmental modifications promoted by *S. tenacissima* tussocks. Similar changes in the sign of the correlation with changes in grain size were found for *G. alypum* and *A. cytisoides*, and for *B. retusum* and the chamaephytes, at the spatial scale defined by the first range when passing from the 5 m × 5 m grid to the 2.5 m × 2.5 m grid. These results highlight the importance of the observational scale when analyzing and interpreting the spatial pattern of plant communities, specially when they are formed by species with contrasting sizes (Bellehumeur et al. 1997). They also agree with previous studies reporting changes in the spatial attributes and pattern of plant communities (He et al. 1994; Bellehumeur et al. 1997; Song et al. 1997) and landscape units (Qi and Wu 1996; Wu et al. 2000; Wu 2004) with changes in grain size.

The results presented here suggest that the LMC is a suitable technique for the spatial analysis of patchy vegetation in semi-arid steppes. When compared to other methodologies commonly employed to analyze the spatial pattern of individual plant species or communities (see Dale 1999 for a recent review), one of its main advantages is the opportunity that it gives plant ecologists to analyze spatial relationships between different species independently at different spatial scales. This feature may reveal patterns that cannot emerge when only the global relationship between species is explored (Perry and Dixon 2002), thus providing more clues on the possible mechanisms that determine the community's structure and function. The methodology used here can also profit from GIS capabilities in data acquisition and manipulation, and can be used for the spatial analysis of vegetation over large geographical areas when data from aerial photographs and satellite imaginary are available. It can analyze the anisotropy in the

spatial pattern in a straightforward way, a feature not evaluated in this study. If information on the environment is also available, the LMC can also be used to test for co-ocurrence in the spatial patterns of species and environmental variables. Further studies are needed to compare the methodology introduced in this paper with other approaches commonly used by plant ecologists, with the aim to fully explore its potential and capabilities for the analysis of plant spatial patterns.

Acknowledgments

We are indebted to Richard Webster, who introduced us in the use of LMC, and corrected an earlier draft of the manuscript. We thank María D. Puche and José García for their help during the fieldwork, and Kerry D. Woods, Philip Dixon, Arnold G. van der Valk and two anonymous referees for helpful comments on the manuscript. Financial support to the first author was provided by FPU and Fulbright fellowships, funded by the

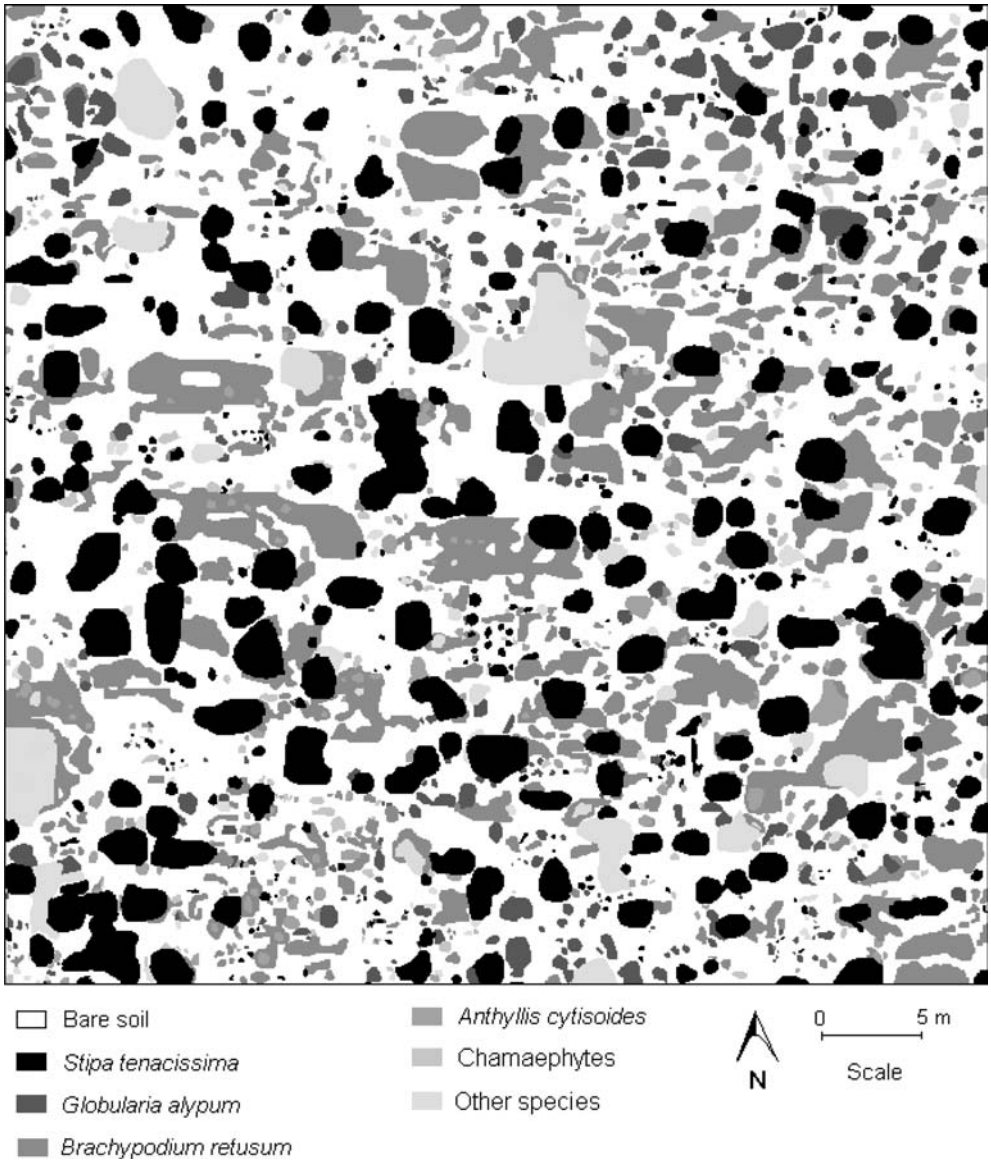

Appendix 1. Digitized map of the 50 m × 50 m steppe studied.

Secretaría de Estado de Educación y Universidades and the Fondo Social Europeo. This is a contribution of the EU-funded REDMED project (ENV4-CT97-0682). CEAM is supported by Generalitat Valenciana and Bancaixa.

References

Allen T.F.H. and Star T.B. 1982. Hierarchy: Perspectives for Ecological Complexity. University of Chicago Press, Chicago.

Anand M. and Kadmon R. 2000. Community-level analysis of spatiotemporal plant dynamics. Ecoscience 7: 101–110.

Bellehumeur C., Legendre P. and Marcotte D. 1997. Variance and spatial scales in a tropical rain forest: changing the size of sampling units. Plant Ecol. 130: 89–98.

Callaway R.M. 1995. Positive interactions among plants. Bot. Rev. 61: 306–349.

Cressie N.E. 1985. Fitting variogram models by weighted least squares. Math. Geol. 17: 563–586.

Dale M.R.T. 1999. Spatial Pattern Analysis in Plant Ecology. Cambridge University Press, Cambridge, UK.

Ehrenfeld J.G., Han X., Parsons W.F.J. and Zhu W. 1997. On the nature of environmental gradients. Temporal and spatial variability of soils and vegetation in the New Jersey Pineland. J. Ecol. 85: 785–798.

García-Fayos P. and Gasque M. 2002. Consequences of a severe drought on spatial patterns of woody plants in a two-phase mosaic steppe of *Stipa tenacissima* L. J. Arid Environ. 52: 199–208.

Greig-Smith P. 1983. Quantitative Plant Ecology. Blackwell, Oxford, UK.

Goovaerts P. 1992. Factorial kriging analysis: a useful tool for exploring the structure of multivariate spatial soil information. J. Soil Sci. 43: 597–619.

Goovaerts P. 1997. Geostatistics for natural resources evaluation. Oxford University Press, New York, USA.

Goulard M. and Voltz M. 1992. Linear coregionalization model: tools for estimation and choice of cross-variogram matrix. Math. Geol. 24: 269–286.

Haase P. 1995. Spatial pattern analysis in ecology based on Ripley's K-Function: introduction and methods of edge correction. J. Veg. Sci. 6: 575–582.

Halpern C. 1988. Early successional pathways and the resistance and resilience of forest communities. Ecology 69: 1703–1715.

Harper J.L., Williams J.T. and Sagar G.R. 1965. The heterogeneity of soil surfaces and its role in determining the establishment of plants from seed. J. Ecol. 53: 273–286.

He F., Legendre P., Bellehumeur C. and LaFrankie J.V. 1994. Diversity pattern and spatial scale: a study of a tropical rain forest of Malaysia. Environ. Ecol. Stat. 1: 265–286.

Isaaks E.H. and Srivatsava M.R. 1989. An Introduction to Applied Geostatistics. Oxford University Press, New York.

Kotz S., Balakrishnan N. and Johnson N. 2000. Continuous Multivariate Distributions, Vol. 1, Models and Applications, 2nd ed. Wiley-Interscience, New York.

Lechowicz M.J. and Bell G. 1991. The ecology and genetics of fitness in forest plants, part 2. Microspatial heterogeneity of the edaphic environment. J. Ecol. 79: 687–696.

Levin S.A. 1992. The problem of pattern and scale in ecology. Ecology 73: 1943–1967.

Le Houérou H.N. 2001. Biogeography of the arid steppeland north of the Sahara. J. Arid Environ. 48: 103–128.

Maestre F.T., Bautista S. and Cortina J. 2003. Positive, negative and net effects in grass-shrub interactions in semiarid Mediterranean steppes. Ecology 84: 3186–3197.

Maestre F.T. and Cortina J. 2002. Spatial patterns of surface soil properties and vegetation in a Mediterranean semi-arid steppe. Plant Soil 241: 279–291.

Maestre F.T. and Cortina J. 2004. Insights on ecosystem composition and function in a sequence of degraded semiarid steppes. Restoration Ecol. 14: 494–502.

Maestre F.T., Huesca M.T., Zaady E., Cortina J. and Bautista S. 2002. Infiltration, penetration resistence and microphytic crust composition in contrasted microsites within a Mediterranean semi-arid steppe. Soil Biol. Biochem. 34: 895–898.

Mateo G. and Crespo M.B. 1998. Manual para la determinación de la flora valenciana. Monografías de flora Montibérica n° 3. Alicante.

Pannatier Y. 1997. Variowin Software for Spatial Data Analysis in 2D. Springer Verlag, New York, NY.

Perry J.N. and Dixon P. 2002. A new method to measure spatial association for ecological count data. Ecoscience 9: 133–141.

Perry J.N., Liebhold A.M., Rosenberg M.S., Dungan J.L., Miriti M., Jakomulska A. and Citron-Pousy S. 2002. Illustrations and guidelines for selecting statistical methods for quantifying spatial pattern in ecological data. Ecography 25: 578–600.

Puigdefábregas J. and Sánchez G. 1996. Geomorphological implications of vegetation patchiness on semi-arid slopes. In: Anderson M.G. and Brooks S.M. (eds), Advances in Hillslope Processes, vol. 2. John Willey and Sons, London, pp. 1027–1060.

Puigdefábregas J., Solé-Benet A., Gutiérrez L., Del Barrio G. and Boer M. 1999. Scales and processes of water and sediment redistribution in drylands: results from the Rambla Honda field site in Southeast Spain. Earth-Sci. Rev. 48: 39–70.

Qi Y. and Wu J. 1996. Effects of changing scale on the results of landscape pattern analysis using spatial autocorrelation indices. Landscape Ecol. 11: 39–50.

Rivera D. and Obón C. 1991. La guía de incafo de las plantas útiles y venenosas de la Península Ibérica y Baleares (excluidas medicinales). Editorial Incafo, Madrid.

Robertson G.P. and Freckman D.W. 1995. The spatial distribution of nematode trophic groups across a cultivated ecosystem. Ecology 76: 1425–1432.

Rossi R.E., Mulla D.J., Journel A.G. and Franz E.H. 1992. Geostatistical tools for modeling and interpreting ecological spatial dependence. Ecol. Monogr. 62: 277–314.

Shipley B.D. and Keddy P.A. 1987. The individualistic and community-unit concepts as falsifiable hypotheses. Vegetatio 69: 47–55.

Soil Survey Staff. 1990. Keys to Soil Taxonomy, 4th ed. Soil Management Support Services technical monograph No. 6, Blacksburg, Virginia.

Song B., Chen J., Desanker P.V., Reed D.D., Bradshaw G.A. and Franklin J.F. 1997. Modelling canopy structure and heterogeneity across scales: From crowns to canopy. For. Ecol. Manage. 96: 217–229.

Turner M.G., Dale V.H. and Gardner R.H. 1989. Predicting across scales: theory development and testing. Landscape Ecol. 3: 245–252.

Valentin C., d'Herbes J.M. and Poesen J. 1999. Soil and water components of banded vegetation patterns. Catena 37: 1–24.

Verdú M. and García-Fayos P. 1998. Old-field colonization by *Daphne gnidium*: seedling distribution and spatial dependence at different scales. J. Veg. Sci. 9: 713–718.

Webster R., Atteia O. and Dubois J.P. 1994. Coregionalization of trace metals in the soil in the Swiss Jura. Eur. J. Soil Sci. 45: 205–218.

Webster R. and Maestre F.T. 2004. Spatial analysis of semi-arid patchy vegetation by the cumulative distribution of patch boundary spacings and transition probabilities. Environ. Ecol. Stat. 11: 257–281.

Webster R. and Oliver M.A. 1990. Statistical Methods for Land Resource Survey. Oxford University Press, Oxford, UK.

Werner B.T. 1999. Complexity in natural landform patterns. Science 284: 102–104.

Wu J. 1999. Hierarchy and scaling: extrapolating information along a scaling ladder. Can. J. Remote Sens. 25: 367–380.

Wu J. 2004. Effects of changing scale on landscape pattern analysis: scaling relations. Landscape Ecol. 19: 125–138.

Wu J., Jelinski D.E., Luck M. and Tueller P.T. 2000. Multiscale analysis of landscape heterogeneity: scale variance and pattern metrics. Geogr. Inf. Sci. 6: 6–19.

Wu J. and Loucks O.L. 1995. From balance-of-nature to hierarchical patch dynamics: a paradigm shift in ecology. Q. Rev. Biol. 70: 439–466.